Applied Catalysis B: Environmental 89 (2009) 246–254

Contents lists available at ScienceDirect

Applied Catalysis B: Environmental

journal homepage: www.elsevier.com/locate/apcatb

Mechanistic study of acidic and basic sites for CO oxidation over nano based $Co_{2-x}Fe_xWO_6$ catalysts

A.V. Salker *, S.J. Naik

Department of Chemistry, Goa University, Goa 403206, India

ARTICLE INFO

Article history:
Received 19 January 2009
Received in revised form 4 March 2009
Accepted 19 March 2009
Available online 27 March 2009

Keywords:
Citrate precursor
Cobalt tungstate
Iron tungstate
Temperature programmed desorption
Carbon monoxide oxidation
Acidic sites
Basic sites

ABSTRACT

This paper deals with systematic study of $M^IM^{II}WO_6$ (M^I = Co and M^{II} = Fe) mixed oxide catalysts for carbon monoxide (CO) oxidation. The catalysts were prepared by polymer based citrate sol–gel method and characterized by X-ray diffraction, thermal analysis, infrared spectroscopy, scanning electron microscopy (SEM) and transmission electron microscopy (TEM). The average particle size calculated using TEM studies were found to be in the range 20–40 nm. DC electrical conductivity showed phase transition from extrinsic to intrinsic behaviour. The ammonia and carbon dioxide adsorption over these catalysts surfaces were used as a probe to confirm the acidic and basic sites. The acidic and basic sites ascertained by temperature programmed desorption (TPD) studies carried out using thermogravimetry and differential scanning calorimetry technique. The presence of acidic and basic sites in equal ratio on the catalyst surface exhibited better CO oxidation activity as compared to unequal number of sites. The equal affinity for CO adsorption over acidic and O_2 on basic sites were found to be essential criteria for catalytic CO oxidation reaction.

1. Introduction

Carbon monoxide (CO) is a toxic component of air. Catalytic oxidation of carbon monoxide to carbon dioxide at ambient temperature and pressure is an important process for respiratory protection. The presence of carbon monoxide in the atmosphere results from the industrial and automobile processes, volcanic activity or bushfires. The condition of the environment and the human health are directly related to the anthropogenic emission. There are numerous and different sources of carbon monoxide formation, e.g. transport, energy production, agriculture, chemical and steel industry. One of the most efficient ways of its removal is catalytic combustion. Recently it can be observed as an increased interest of catalytic removal of carbon monoxide at low temperatures. This results from the appearance of new potential applications, e.g. production and purification of hydrogen for fuel cells (preferential oxidation of CO), the need of the improvements of the vehicle catalytic systems, more efficient cleaning of the air or CO removal in the laser devices.

The natural and synthetic tungstate systems reveal the unique structural, electronic, magnetic and catalytic properties. Transition metal tungstates have found wide interest with their potential applications as materials for scintillation detectors, photo anodes, Optical fibers [1] and in the field of catalysis. Among these tungstates, transition metals Co and Fe tungstates have been also studied due to their catalytic activities for hydrodesulphurization of anode, oils fractions [2–4] and propane oxydehydrogenation to propylene [5], metal crystallites, and large inorganic or organic species [6]. The activity of tungsten oxide catalysts has been often improved by the application of different supports, special preparation routes or introduction of transition and noble metals.

Crystalline A_2BO_6 has tri-rutile structure, which is built up of hexagonally close packed oxygen with certain octahedral sites filled by Co^{3+}/Fe^{3+} and W^{6+} cations in an ordered way [6,7]. Their catalytic activity has been strongly related to the synthesis and reaction conditions, including the ageing time, pH, temperature or humidity [8–10]. The exposed cations and anions on oxide surfaces have been described as acid–base site pairs [11]. In the metal oxide systems, oxide ions act as Lewis base site and metal cations as Lewis acid sites. Strong Bronsted acidity usually arises in mixed oxides rather than pure oxides due to charge imbalance or co-ordination changes occurred due to incorporation of second cations. Exposed coordinatively unsaturated cations may act as acceptors for free electron pairs of adsorbed species [11]. The negative charge of the CO molecule is located at the C- end and consequently CO is usually adsorbed via its C-end. The strength of C–O bond depends on the balance between the electrostatic σ- and π-bonds [12].

* Corresponding author. Tel.: +91 832 6519315; fax: +91 832 2451184.
E-mail address: avsalker@gmail.com (A.V. Salker).

0926-3373/$ – see front matter © 2009 Elsevier B.V. All rights reserved.
doi:10.1016/j.apcatb.2009.03.025

The purpose of this study is to understand the catalytic process, the influence of surface acidic as well as basic sites and to see the catalytic activity of CO oxidation under these conditions. The CO oxidation was carried out over Co–Fe–W mixed metal oxides and exposed to surface rich acidic and basic sites. The adsorption and desorption data provide information about the role of acidic and basic sites in CO oxidation. In this work, tungstates were synthesized using a polymeric precursor method which is highly reproducible and low cost compared to other chemical methods of preparation. The method was successfully used in the preparation of nano-particles and is based on the chelation of cations by a hydro carboxylic acid. The various metal compositions of cobalt and iron tungstates were prepared at comparatively lower temperature.

2. Experimental

2.1. Catalyst preparation

For the preparation of $Co_{2-x}Fe_xWO_6$ (x = 0.0, 0.5, 1.0, 1.5 and 2.0), the polymeric precursor method [13] was employed. A tungsten citrate solution was initially prepared, followed by the synthesis of the powder precursor. Preparation of the tungsten citrate solution started with the dissolution of tungstic acid in water at 70 °C at pH 8–9. Citric acid was dissolved in distilled water at the same temperature and this solution was slowly added to the tungstic acid solution. The ensuing tungsten citrate solution was later filtered and subjected to a gravimetric analysis in order to obtain information concerning stoichiometry. For the synthesis of the polymeric resin, citric acid was added to the tungsten citrate solution followed by the addition of cobalt and iron nitrate under constant stirring at around 100 °C. The ensuing resins were calcined at 200 °C for 2 h, leading to the formation of precursor sample, which were grinded in agitate mortar. The samples were then subjected to thermogravimetry and differential scanning calorimetry (TG/DSC) at a flow of 20 ml/min of synthetic air and a heating rate of 10 °C/min up to 1000 °C to find the sintering temperature for the precursors. The precursors were subsequently calcined at 600 °C for 5 h.

The acid and base promoted tungstates were prepared by immersing the catalyst in a solution of 0.005 M HNO_3 and liquor ammonia (25%) separately. The suspension was stirred for 1 h at room temperature, filtered and evaporated to dryness at 110 °C for 5 h. The samples were calcined in air at 400 °C for 2 h.

2.2. Catalyst characterization

The thermal studies of the samples were investigated using thermal techniques (TG/DSC/Netzsch STA49A). Approximately 10 mg of the precursor material was placed in an alumina sample pan. The sample was heated up to 1000 °C with the heating rate of 10 °C/min in flowing synthetic air. The weight loss of the precursor sample at thermal event was recorded during heating. BET surface area was measured at boiling point of liquid nitrogen using a Smartsorb 90/91 instrument. The XRD patterns were recorded using a Rigaku Miniflex Diffractometer with CuKα radiation filtered through Ni absorber. The scanning electron microscopy (SEM) images were obtained using JEOL model 5800LV, Japan Microscope operating at 300 kV. The transmission electron microscopy (TEM) images were taken employing Tecnai F-30 microscope, using an accelerating voltage of 300 kV. Fourier transform infrared (FTIR) spectroscopy analysis was performed with Shimadzu IR prestige 21 spectrometer in diffuse reflectance infrared mode.

2.3. Physical properties

Diffuse reflectance spectra (DRS) were recorded on Shimadzu UV 2450 UV–vis spectrometer in the wave length range of 300–800 nm. For electrical conductivity measurements, the samples in the form of tablets were prepared by compressing with hydraulic press at 10 ton of pressure and sintered at 600 °C for 5 h. Both the sides of the pellet were pasted with silver paste. The pellet was placed between electrodes of two probe conductivity unit. The temperature variation of resistance was measured from room temperature to 400 °C. Conductivity was measured in both heating and cooling cycles. The magnetic properties were determined by Gouy balance and hysteresis loop tracer methods. The Gouy method was used to measure magnetic susceptibility at room temperature with a field of the order 8500 G using mercury tetrathiocyanatocobaltate ($Hg[Co(SCN)_4]$) as the standard material, whereas saturation magnetization was carried out using nickel as standard material employing hysteresis loop tracer.

2.4. Temperature programmed desorption

Temperature programmed desorption (TPD) studies were performed using thermal analysis technique. The adsorption of NH_3 and CO_2 were carried out at 40 °C. For the NH_3 adsorption a flow of NH_3 and N_2 mixture for half an hour was obtained by passing N_2 through a saturator containing liquid ammonia at room temperature. After adsorption the sample was purged with N_2 (40 ml/min) till it attains room temperature. The gas desorption studies of the catalysts were monitored by thermal analyzer indicating weight loss at desorption temperature and showing endothermic or exothermic peaks in the DSC curve. Similarly, desorption of CO_2 was also monitored by using thermal analyzer.

2.5. Catalytic studies

Catalytic reactions were conducted in a continuous flow fixed bed glass reactor. About 1.0 g of the catalyst was loaded and sandwiched between two layers of glass wool. Before the reaction, the catalyst was activated with oxygen (250 ml/h) in N_2 at 150 °C for half an hour. The catalytic activity was determined using a feed gas composition of 5% CO, 5% O_2 in nitrogen. The individual gas flow rates were controlled using flow meters and precision needle valves. The effluent from the reactor was analyzed by an online gas chromatography. Nitrogen, oxygen and carbon monoxide were separated by a packed column molecular sieve 13X and analyzed by thermal conductivity detector (TCD) using H_2 as a carrier gas. The CO was prepared by standard procedure and was purified by passing through appropriate traps [14]. The N_2 and O_2 gases were used from commercial pure cylinders.

3. Results

3.1. Thermal analysis

Thermal analysis was performed for unfinished compounds to find the sintering temperature using TG/DSC. All samples showed the thermal decompositions in two stages. The first step is attributed to the elimination of water, adsorbed gases and the second one is due to the exothermic decomposition of the organic ligands releasing CO_2 and H_2O [13]. The second TG/DSC profile showed greater mass loss and strong exothermic peak. All subsequent discussions will be confined to the analysis of the samples calcined at 600 °C for 5 h.

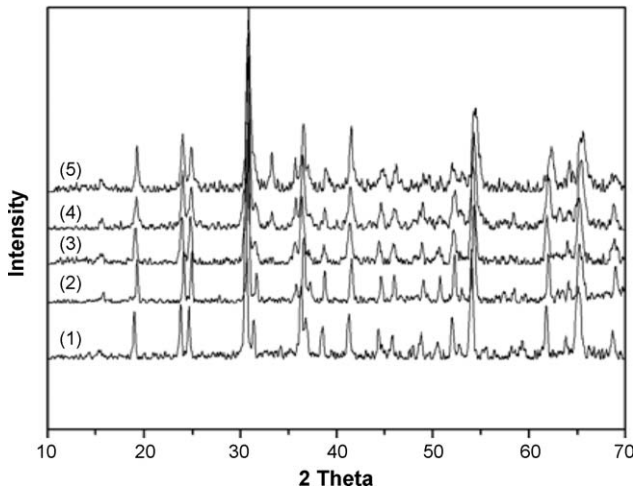

Fig. 1. X-ray powder diffraction pattern of $Co_{2-x}Fe_xWO_6$: (1) Co_2WO_6 (2) $Co_{1.5}Fe_{0.5}WO_6$, (3) $Co_{1.0}Fe_{1.0}WO_6$, (4) $Co_{0.5}Fe_{1.5}WO_6$ and (5) Fe_2WO_6.

3.2. Structural properties of the $Co_{2-x}Fe_xWO_6$ catalyst

Fig. 1 shows the XRD pattern of the $Co_{2-x}Fe_xWO_6$ compositions. From the X-ray diffraction pattern, it was confirmed that the tungstate forms tri-rutile structure. Since the *d*-spacing of the intermediate compositions (x = 0.5, 1.0 and 1.5) are not reported in the literature, the values were compared with the end compositions namely Co_2WO_6 and Fe_2WO_6 [15,16].

Scanning electron microscopy of $Co_{2-x}Fe_xWO_6$ compounds, with x = 0.0, 1.0 and 2.0 calcined at 600 °C is shown in Fig. 2a. From these images it is inferred that the morphology of the particles size decreases with increase in the Fe content. The sample with x = 0 shows particles of non-uniform size and shape as compared to that of the sample with x = 1.0. This may be due to the aggregation of particles with increase in cobalt content whereas well dispersed phase was observed in x = 1.0. It can be concluded that sample with low cobalt favour the formation of fine tungstate particles. To confirm finer details, the TEM images of selective samples were taken and shown in Fig. 2b. From TEM studies the particle sizes are ranged from 20 nm to 40 nm.

3.3. BET surface area analysis

The BET surface areas of $Co_{2-x}Fe_xWO_6$ compounds after calcination were in the range 3.5–9.8 m^2/g. It was observed that the surface area of the tungstate increases with increase in Fe content although the methods of sample preparation were identical.

3.4. Fourier transformation infrared spectroscopy

IR spectroscopic studies were carried out in order to investigate the nature of metal–oxygen bonding present in the Co–Fe–W–O

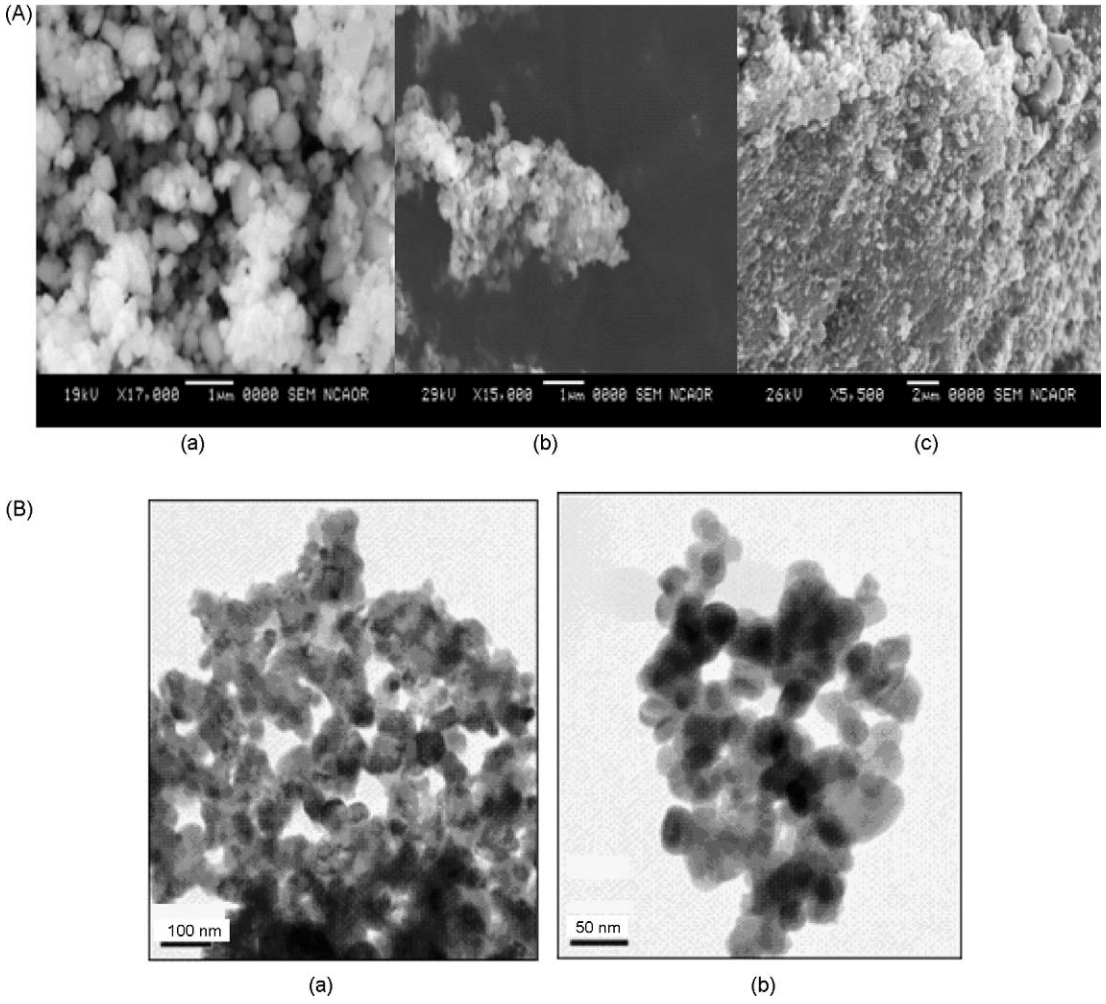

Fig. 2. (A) SEM Photographs of the compounds prepared at 600 °C, (a) Co_2WO_6 (b) $Co_{1.0}Fe_{1.0}WO_6$ and (c) Fe_2WO_6. (B) TEM photographs (a) $Co_{1.0}Fe_{1.0}WO_6$ and (b) Fe_2WO_6.

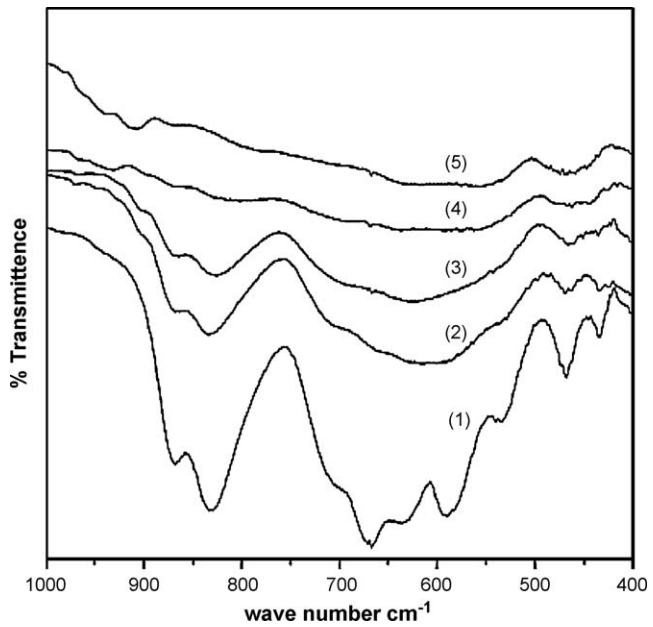

Fig. 3. FTIR spectra of $Co_{2-x}Fe_xWO_6$ series, (1) Co_2WO_6 (2) $Co_{1.5}Fe_{0.5}WO_6$ (3) $Co_{1.0}Fe_{1.0}WO_6$ (4) $Co_{0.5}Fe_{1.5}WO_6$ and (5) Fe_2WO_6.

system. A_2BO_6 structure is known to be characterized by IR spectra. The IR spectra of the mixed metal oxides show strong absorption bands at 900–400 cm^{-1} corresponding to the strong vibrations of the metal-oxygen bonds as shown in Fig. 3. Results showed that the bands in the range 800–900 cm^{-1} regions can be attributed to the symmetric and asymmetric stretching vibrations of W–O bonds in joint WO_6 octahedra [17]. Moreover the structure has a relatively high degree of condensation of oxygen atoms around W^{6+} ions and dense packing of the condensation polyhedra, in the unit cell. The resulting co-ordination number (CN) is six, because the tungstate ions are additionally connected to each other by means of intra-molecular (w:w) (tungsten–tungsten bridge bond) type interactions. Characteristic vibrational bands correspond to the stretching modes of (w:w) units [18–21]. The bands at 870 and 830 cm^{-1} assigned to the symmetric stretching of WO_6, leads to the conclusion that there is only one type of WO_6 unit. The corresponding bending vibrations were located in the 400–450 cm^{-1} region. Stretching vibrations of the longer W–O bonds which take part in the formation of (w:w) (second type of tungsten–tungsten bridge bond) bridges were observed in the 450–700 cm^{-1} region. The substitution of Co by Fe in the tri-rutile type compounds produced significant shift in the IR bands, in particular υ_{as} stretch of the Co–O band peak shifted from 680 cm^{-1} to higher frequency. The absorption bands occurring in the IR–spectra of $Co_{2-x}Fe_xWO_6$ compounds below 500 cm^{-1} may be attributed to the deformation modes of W–O bonds in the WO_6 octahedra or deformation of W–O–W bridges [16]. The literature data [18] were compared to the bands observed in the present work. For the majority of the bands, no meaningful vibration was observed, when Fe^{3+} was substituted for Co^{3+}. Only two bands present a variation in their positions namely the υ_{as} (WO_6) and υ_{as} (w:w) stretching modes between 800–700 cm^{-1} and the $\delta[WO_6]$ bending mode, which varied from 400–500 cm^{-1}. These bands are probably influenced by the bonding amongst [WO_6] and the [FeO_6] or [CoO_6] octahedral [17].

3.5. Diffuse reflectance UV–vis spectra

The diffuse reflectance spectra of $Co_{2-x}Fe_xWO_6$ samples were recorded at room temperature as shown in Fig. 4. Some of these

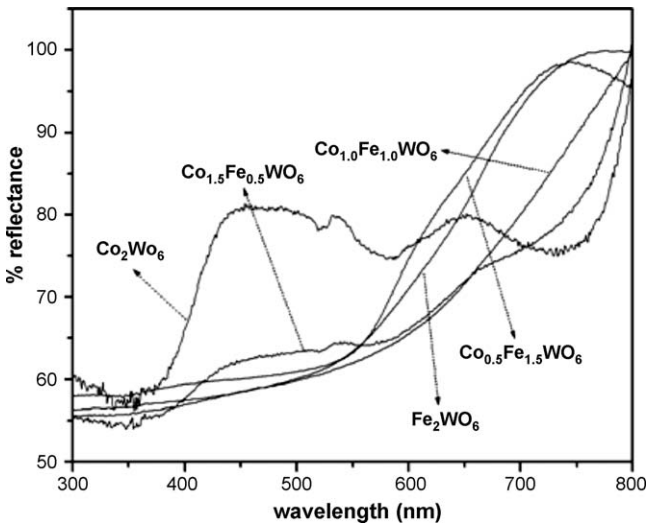

Fig. 4. Diffuse reflectance spectra of $Co_{2-x}Fe_xWO_6$ compounds.

compounds did not show any sharp drop in energy, indicating that they are not good semiconductors as in x = 0.0 and 0.5, whereas the compositions x = 1.5 and 2.0 at room temperature showed definite drop in energy in DRS spectra indicating that these compounds are good semiconductors. This is also reflected in electrical conductivity measurements as shown in Fig. 5. Some of these compounds show absorption bands indicating that they are colour pigments.

3.6. Electrical properties

Electrical conductivity (σ) of tungstates was measured using two probe method from room temperature to 450 °C in air. Ohmic contacts to the pallet sample were made with silver paste. Fig. 5 shows a plot of log σ verses inverse of absolute temperature ($1/T$) and σ is expressed as given below:

$$\sigma = \sigma_o \exp(-E_a/2KT)$$

where E_a is the activation energy and other symbols have their usual meanings. It was observed that the conductivity decreases with increase in temperature for the compositions x = 0.0, 0.5, and 1.0. For these the decrease in the range from room temperature

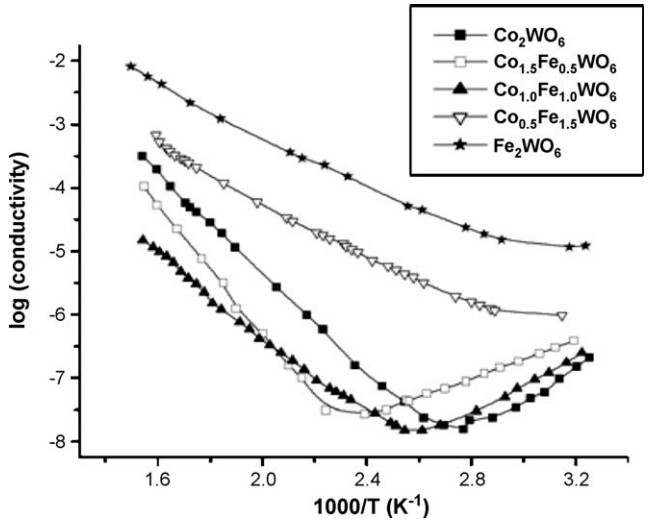

Fig. 5. Temperature variation of electrical conductivity of $Co_{2-x}Fe_xWO_6$ compounds during cooling cycle.

Table 1
Surface area, CO conversion and saturation magnetization of the compounds.

Catalyst	Surface area (m^2/g) (prepared at neutral pH)	Light off temperature (50% CO conversion) (T °C)	$T_{100\%}$ (100% CO conv.)	(μ_s) Saturation magnetization (emu/g)
Co_2WO_6	6.6	127	139	Paramagnetic
$Co_{1.5}Fe_{0.5}WO_6$	3.5	142	160	1.13
$Co_{1.0}Fe_{1.0}WO_6$	6.5	155	171	0.55
$Co_{0.5}Fe_{1.5}WO_6$	7.9	211	280	4.48
Fe_2WO_6	9.8	247	310	4.78

(RT) to 200 °C followed by the increase in conductivity. But for the compositions $x = 1.5$ and 2.0 conductivity increases with increases in temperature as normal semiconductors. It is suspected that a phase transition from extrinsic to intrinsic type semiconductivity in $x = 0.0$, 0.5 and 1.0 compounds. The measurements were repeated on the same set as well as different sets of samples thrice and observed the same trends of conductivity behaviour in ambient air. It can be seen from the Fig. 5, that the discontinuity in the curve occurs at around 200 °C, this low temperature decrease in conductivity may be considered as extrinsic behaviour, whereas conduction in the higher temperature region may be regarded as intrinsic [22]; therefore the change in the slope of the plot of log σ vs (1/T) is attributed to the change in the conduction mechanism. It is suspected that the moisture from air also influencing the conduction of the samples. From DRS study the compositions $x = 0.0$ and 0.5 show absorption bands, whereas $x = 1.5$ and 2.0 show linear fall in the energy, indicating that they are room temperature semiconductors.

3.7. Magnetic studies

The magnetic susceptibility (χ) and saturation magnetization (μ_s) values were determined at room temperature. Compound Co_2WO_6 is paramagnetic at room temperature, with magnetic susceptibility value 42.32×10^{-6} cgs units whereas all the other compounds are antiferromagnetic in nature. The magnetic values were studied by the saturation magnetization method. The saturation magnetization emu/g increases with the Fe content as shown in Table 1. The Fe_2WO_6 shows highest saturation magnetization than other compositions, due to the strong antiferromagnetic nature of the compounds [6,7].

3.8. Temperature programmed desorption of ammonia (TPD-NH_3)

Ammonia is used as a probe to determine the acidity of the catalyst. Being small in size ammonia can penetrate into the pores of tungstates and interact with Bronsted and Lewis acid sites. TPD of ammonia is a good technique for rapid characterization of acidity of mixed metal oxides. The low temperature peak was assigned to the desorption of NH_3 on weak acid sites whereas the high temperature peak was assigned to desorption of the chemisorbed NH_3 from strong Bronsted acid sites [23]. There is a loss of strong acidity at high temperature may be due to sintering. This disappearance of high temperature peak indicates that the cobalt oxides migrated into the channels of the iron oxide and preferentially interacted with strong acids [24]. The concentration of strong basic sites decreased with increase in Fe loading in Co_2WO_6. In these experiments the acid and base treated Co_2WO_6 showed weight loss at desorption temperature as seen in Fig. 6(a). The acid treated Co_2WO_6 showed an endothermic peak at 92 °C and exothermic peak at 212 °C in the DSC plot. The endothermic peak is due to the surface adsorbed water, whereas the exothermic peak is due to desorption of ammonia from the catalyst surface. In the same way the acid as well as base treated Fe_2WO_6 compound, TPD–NH_3 studies were carried out, but the weight loss in TG and exothermic peak in DSC are weak as seen in Fig. 6(b), indicating that the acidic and basic sites are less compared to Co_2WO_6 compounds.

3.9. Temperature programmed desorption of carbon dioxide (TPD-CO_2)

The basicity of $Co_{2-x}Fe_xWO_6$ was measured by means of TPD-CO_2 and the results are shown in Fig. 7(a) and (b). The TPD of CO_2 shows three main events at three different temperature range i.e. low basicity sites where CO_2 is desorbed within the temperature range of 80–140 °C, medium basicity sites within the range of 160–240 °C and high basicity sites where CO_2 is desorbed at around 300 °C. It was understood that these difference in desorption temperatures is due to the basic strength of the catalyst surface [25,26]. For example, CO_2 adsorbed on low basic sites which are related to OH^- groups on the catalyst is desorbed at around 100 °C. The medium strength of the basicity is related to the oxygenated ion of $2Co^{3+}\cdots3O^{2-}$ and $2Fe^{3+}\cdots3O^{2-}$ [27,28]. The strong basicity is not visible clearly in either TG or DSC peaks. It may be conclude that the strong basicity is weaker in these compounds. The strong

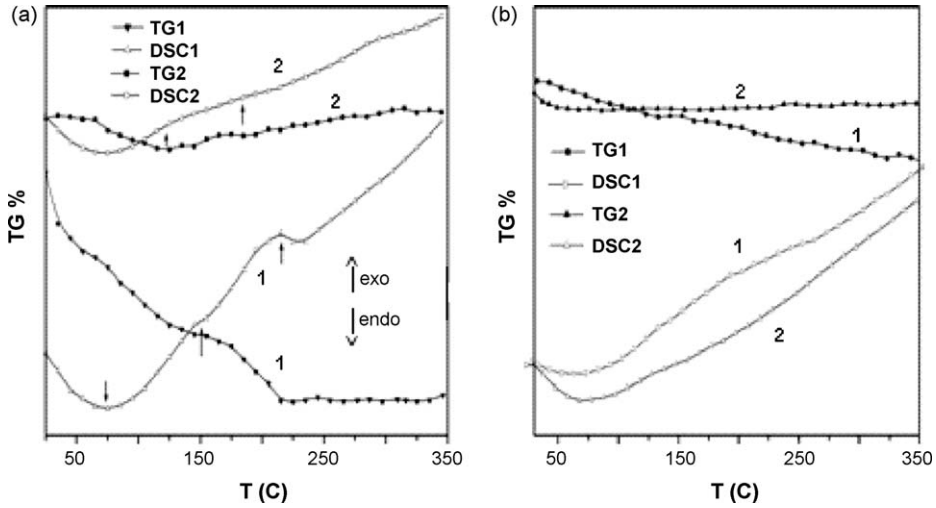

Fig. 6. (a) Temperature programmed desorption of NH_3 using TG/DSC, (1) Co_2WO_6 acid treated NH_3 desorption and (2) Co_2WO_6 base treated NH_3 desorption. (b) Temperature programmed desorption of NH_3 using TG/DSC, (1) Fe_2WO_6 acid treated NH_3 desorption and (2) Fe_2WO_6 base treated NH_3 desorption.

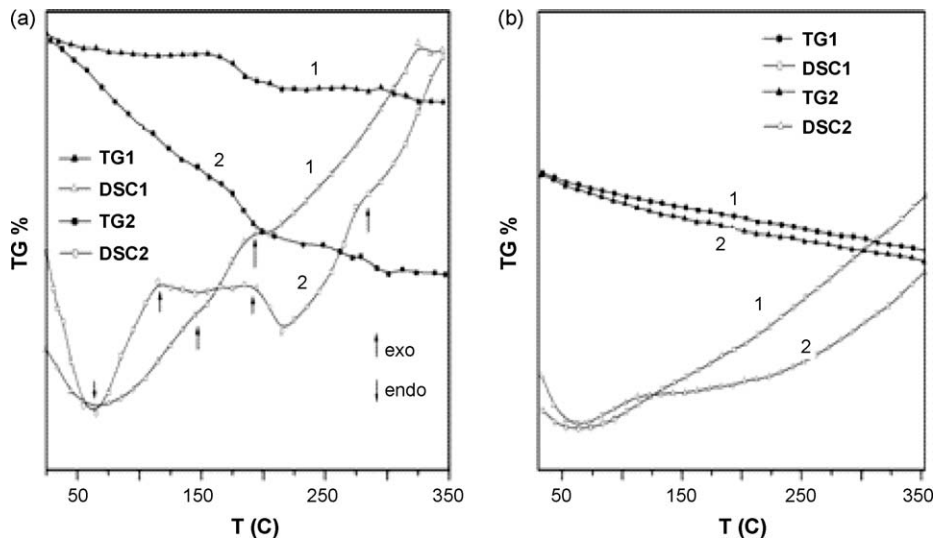

Fig. 7. (a) Temperature programmed desorption of CO_2 using TG/DSC, (1) Co_2WO_6 acid treated CO_2 desorption and (2) Co_2WO_6 base treated CO_2 desorption. (b) Temperature programmed desorption of CO_2 using TG/DSC, (1) Fe_2WO_6 acid treated CO_2 desorption and (2) Fe_2WO_6 base treated CO_2 desorption.

basicity is associated with the O^{2-} in the lattice of $Co_{2-x}Fe_xWO_6$ compounds. The TPD-CO_2 profiles obtained were different over these catalysts. The medium basicity peak was observed in the range of 180–210 °C in acid treated Co_2WO_6 with corresponding weight loss in TG peak and exothermic peaks in DSC. In base treated sample, exothermic peaks are observed at 210, 260 and 300 °C showing medium and strong basicity. In case of Fe_2WO_6 base treated sample exothermic peaks were observed at 190 and 210 °C showing medium basicity. The weight loss and exothermic peaks are not conspicuous, indicating poor medium basicity in the catalyst. Whereas in case of acid treated sample, no amount of weight loss and exothermic peaks were observed, thus concluding that the basic sites are almost absent on Fe_2WO_6 catalyst. Therefore, Fe_2WO_6 may show poor CO oxidation activity. This concept is confirmed by the observations in CO oxidation results.

3.10. Catalytic oxidation of carbon monoxide

In order to compare the catalytic activity the CO oxidation was carried out over acid and base enriched catalysts. Figs. 8–10 show the CO oxidation over acid enriched, base treated and as such prepared $Co_{2-x}Fe_xWO_6$ compounds respectively. It was observed that the incorporation of Fe in the lattice of Co_2WO_6 showed a significant change in the catalytic activity. For the catalytic oxidation reaction both reactants should adsorb over the catalyst surface. It is found that the carbon monoxide has excess electrons and it requires acidic sites to get adsorb, similarly for oxygen basic sites are needed. Therefore, for complete oxidation both acidic and basic sites on the catalyst surface are essential. The acid enriched catalysts showed high CO conversion at lower temperatures, this is due to the presence of sufficient active acidic and basic sites on the catalyst surface. Subsequently base treated sample does not show much conversion as compared to acid treated catalysts because of unequal number of acidic and basic sites. It confirmed from TPD studies that the base treated catalysts contain less number of acidic sites and it fail to adsorb more CO on the surface. But on as prepared catalyst there is some acidic and basic sites, this is the reason why it showed some activity. For maximum catalytic activity it is essential both surface rich acidic and basic sites in equal ratio on the surface.

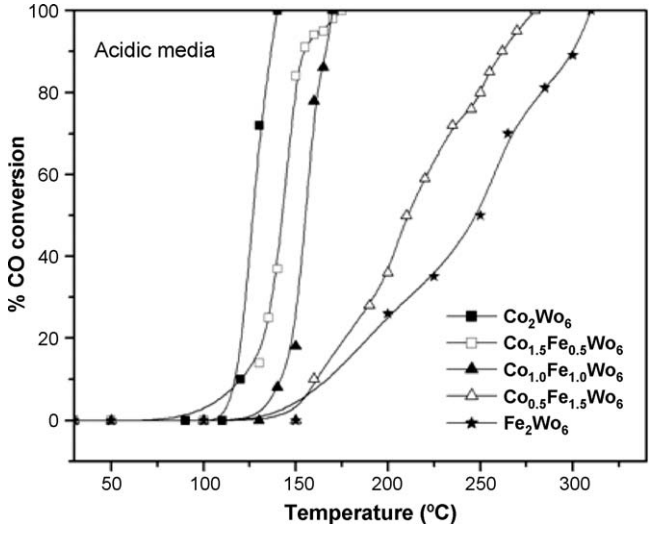

Fig. 8. Carbon monoxide oxidation over acid treated compounds.

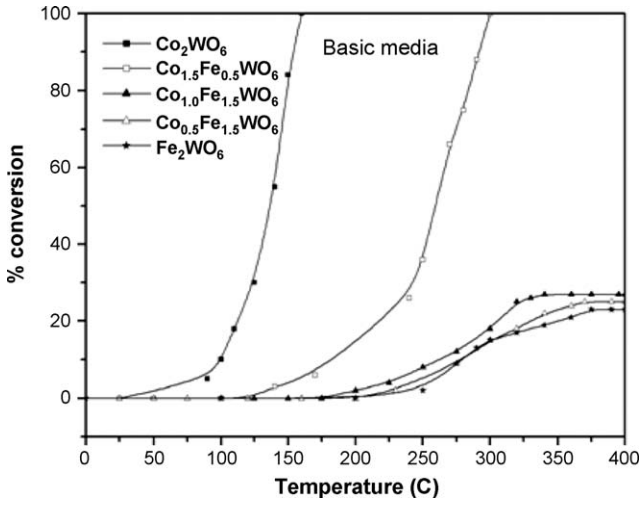

Fig. 9. Carbon monoxide oxidation over base treated compounds.

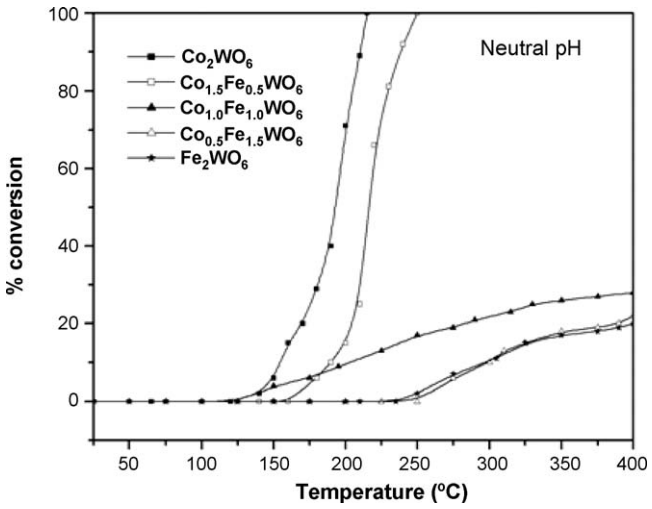

Fig. 10. Carbon monoxide oxidation over as such prepared compounds.

4. Discussion

Adsorption of CO on acidic and oxygen on basic sites are accompanied by charge transfer mechanism. It can be said that lone pair of electrons from the carbon hybrid sp_z will be accommodated by an empty d-orbital of the metal, thus creating a σ-bond. This bond is stabilized by back transfer of electrons from the filled d-orbital of the metal to the empty antibonding $2\pi^*$ orbital of the CO molecule.

4.1. CO oxidation over acid treated catalysts

Fig. 8 shows the CO oxidation over the acid enriched $Co_{2-x}Fe_xWO_6$ catalysts. For Fe_2WO_6, the induction temperature for CO oxidation was high as compared to the other compositions. The temperature programmed desorption studies of NH_3 and CO_2 confirm that Co_2WO_6 having both acidic and basic sites on the same catalyst. But the Fe_2WO_6 has only acidic sites from the TPD–NH_3 study, whereas the basic sites are almost absent on the catalyst surface and this may inhibit the adsorption of oxygen molecule, therefore, expected to show poor activity. Decomposition of nitrate during the preparation of the compounds releases NO_2 gas making the catalyst surface rich in oxygen, i.e. $NO_3^- \rightarrow NO_{2(g)} + O^-$. These surface oxygen atoms may help carbon monoxide to get oxidized. This may be one of the reasons for the slight activity of Fe_2WO_6. From Fig. 10 it is clear that as Fe content increases in the Co_2WO_6 the catalytic activity decreases.

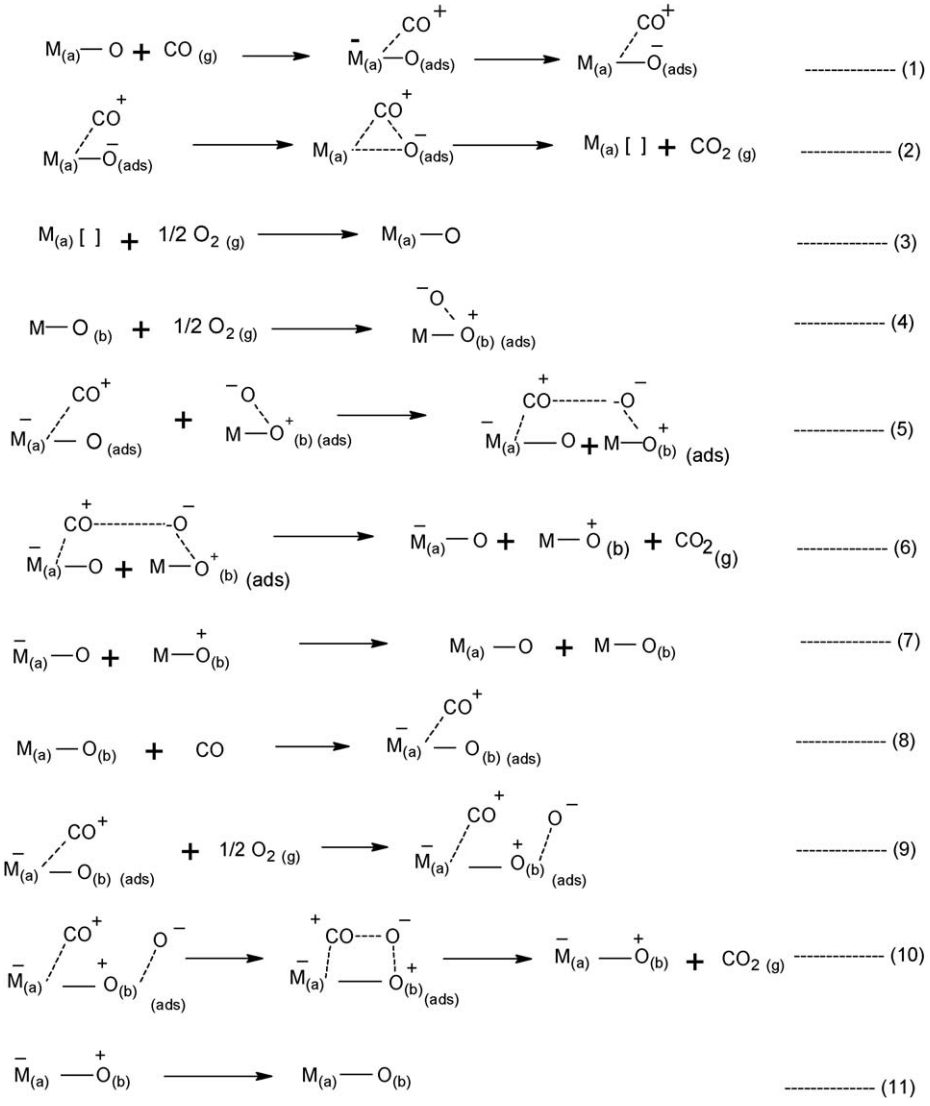

Scheme 1.

4.2. CO oxidation over base treated catalysts

Fig. 9 shows the CO oxidation over the base treated catalysts. The Co_2WO_6 showed high activity, due to presence of both acidic and basic sites. But the quantity of acidic sites is less as compared to the acid treated sample. The acid treated catalyst showed 100% CO conversion at 130 °C whereas, the base treated showed at 150 °C. The same is observed for $Co_{1.5}Fe_{0.5}WO_6$ catalyst, where the activity decreases from 170 °C to 280 °C for 100% conversion to the base treated sample. The other compositions showed lower activity. For these catalysts the excess of basic sites are available for O_2 adsorption, but the CO is not adsorbed on the surface due to unavailability of acidic sites hence the activity decreases. The concentrations of acidic and basic sites are indicated in the TPD curves.

4.3. CO oxidation over as prepared catalysts (without acid–base treatment)

As prepared compounds showed the similar CO oxidation pattern as that of the base treated sample as shown in Fig. 10. For the preparation of the catalyst, organic acid is used as a chelating agent. This citric acid precursor tends to make the surface more acidic. It was observed that concentrations of acidic sites were less as compared to the acid treated sample. The activity of Co_2WO_6 decreased compared to acid and base treated samples. As Fe content increases the availability of basic sites decreases. The TPD studies showed that the compounds are acidic hence carbon monoxide adsorption takes place over the catalyst, but it fails to get the equal amount of oxygen over the surface due to less number of basic sites. There is lack of electrons over the surface for oxygen molecule to get adsorbed. The cobalt tungstate tries to maintain the acidic and basic sites in equal ratio in both acidic and basic conditions. Therefore, the acid and base treatment is not much affected on the cobalt containing compounds, on the contrary showed higher CO oxidation reaction.

4.4. Reaction mechanism

The oxidation of CO on the acidic and basic sites of the catalyst involve a few steps such as intraparticle diffusion, adsorption of the reactants, reaction of the adsorbed species and desorption of the products. Some investigators have attempted to propose the reaction mechanism of CO oxidation [29,30]. Scheme 1 shows the reaction path ways based on the investigations. This is analogous in parts to those proposed by others and is one of the possible reaction path ways.

Here $M_{(a)}$–O and $M_{(b)}$–O are considered as two types of active sites on metal oxides namely acidic and basic sites respectively. Where $M_{(a)}$ as surface active acidic site and $O_{(b)}$ as basic active site on metal oxides. $M_{(a)}$ is considered as an acidic site which is electron deficient. CO having lone pair of electrons directing the C-end of CO gets chemisorbed with acidic site of metal oxide to form a bond as shown in Eq. (1). The adsorbed CO interacts with the lattice oxygen of the metal oxide. The partially bonded CO_2 gets desorbed leaving the reduced acidic metal oxide on the surface as shown in Eq. (2). Subsequently reduced site takes oxygen from the gas phase to fill the oxygen vacancy as seen in Eq. (3). The oxygen molecule takes electrons from the basic site forming O^- species in Eq. (4). The adsorbed species may interact to give intermediate as shown in Eq. (5), subsequently giving CO_2 and regeneration of the catalyst in Eqs. (6) and (7). If acidic and basic sites are present on the same metal oxide, then the reaction paths ways follow as below. The Eq. (8) indicates the presence of both acidic and basic sites on the same metal oxide. The carbon monoxide adsorbed on the acidic site and oxygen on basic site to form intermediate as shown in Eq. (9) and finally CO_2 gas will desorbs as in Eq. (10), regenerating the active sites as seen in Eq. (11). The above mechanism is in agreement with other investigators in some form or other.

The Co_2WO_6 and $Co_{1.5}Fe_{0.5}WO_6$ in spite of low surface areas and low electrical conductivity showed higher catalytic activity as compared to Fe_2WO_6 and $Co_{0.5}Fe_{1.5}WO_6$ respectively. However, as mentioned earlier Co_2WO_6 and $Co_{1.5}Fe_{0.5}WO_6$ have both sufficient acidic as well as basic sites required for CO oxidation as shown in TPD studies. Thang et al. [31], also observed that the samples with high conductivity will have high catalytic activity is not true, it is also reflected in this observation. Fe_2WO_6 and $Co_{0.5}Fe_{1.5}WO_6$ have higher saturation magnetization than other compounds whereas Co_2WO_6 is paramagnetic. It may be attributed that higher the magnetization value lower is the catalytic activity in this series of compounds. This may be one of the factors influencing CO oxidation rate.

5. Conclusions

Simple soft chemical process has been developed for the preparation of various nano sized metal tungstate powders from a polymer based metal complex precursor solution. Compound $x = 1.5$ and 2.0 at room temperature are semiconductors, whereas $x = 0.0$, 0.5 and 1.0 are showing extrinsic to intrinsic behaviour. The particle sizes are below 40 nm sizes as seen from TEM studies. Temperature programmed desorption of NH_3 and CO_2 provided the qualitative information about the concentration and strength of the acidic and basic sites exposed on the catalyst surfaces. The observation of acidic and basic sites from TPD-NH_3 and TPD-CO_2 plots from TG/DSC studies suggested the possible presence of acidic sites in as such prepared samples and more basic sites in base treated sample. All acid treated samples show high CO oxidation rate, but no significant good activity is observed in Fe containing compounds. The cobalt containing compounds showed higher activity due to equal ratio of acidic and basic sites. It has been found that the density of acidic sites, basic sites, surface area, number of unpaired electrons and surface lattice defects play important roles in CO oxidation over the catalyst.

Acknowledgement

This work is supported by University Grant Commission, New Delhi.

References

[1] O.A. Serra, S.A. Cicilhini, R.R. Ishiki, J. Alloys Compd. 316 (2000) 303, doi:10.1016/S0925-8388(00)00595-8.
[2] B. Grobelna, J. Alloys Compd. 440 (2007) 265, doi:10.1016/j.jallcom.2006.09.012.
[3] F.J. Gil-Lambias, H. Rodriguez, I. Bouyssiers, M. Escudey, I. Carkovic, J. Catal. 102 (1986) 37, doi:10.1016/0021-9517(86)90138-7.
[4] B. Scheffer, P. Molhoek, J.A. Moulijin, Appl. Catal. 46 (1989) 11, doi:10.1016/S0166-9834(00)81391-3.
[5] D.L. Stern, R.K. Grasselli, J. Catal. 167 (1997) 570, doi:10.1006/jcat.1997.1568.
[6] N. Guskos, L. Sadlowski, J. Typek, V. Likodimos, H. Gamari-Seale, B. Bojanowski, M. Wabia, J. Walczak, I. Rychlowska-Himmel, J. Solid State Chem. 120 (1995) 216, doi:10.1006/jssc.1995.1401.
[7] H. Leiva, R. kershaw, K. Dwight, A. Wold, J. Solid. State Chem. 47 (1983) 293, doi:10.1016/0022-4596(83)90021-X.
[8] C.R. Jung, A. Kundu, S.W. Nam, Ho-In Lee, Appl. Catal. B 84 (2008) 426, doi:10.1016/j.apcatb.2008.04.024.
[9] L. Piccolo, H. Daly, A. Valcarcel, F.C. Meunier, Appl. Catal. B 86 (2009) 190, doi:10.1016/j.apcatb.2008.08.011.
[10] F. Romero-Sarria, A. Penkova, L.M.T Martinez, M.A. Centeno, K. Hadjiivanov, J.A. Odriozola, Appl. Catal. B 84 (2008) 119, doi:10.1016/j.apcatb.2008.03.010.
[11] A. Beilanski, J. Haber, Oxygen in Catalysis, 3rd ed., Marcel Dekker, Inc., New York, 1991, p. 159.
[12] K. Hadjiivanov, A. Penkova, M.A. Centeno, Catal. Comm. 8 (2007) 1715, doi:10.1016/j.catcom.2007.02.002.
[13] A.L.M. de Oliveira, J. Ferreira, M. Silva, G. Braga, L. Soledade, M. Aldeiza, C. Paskocimas, S. Lima, E. Longo, A. De Souza, I. Santos, Dyes Pigments 771 (2008) 210, doi:10.1016/j.dyepig.2007.05.004.
[14] A.V. Salker, S.M. Gurav, J. Mater. Sci. 35 (2000) 4713.
[15] J. Walczak, I. Himmel, Thermochem. Acta 239 (1994) 269, doi:10.1016/0040-6031(94)87073-X.

[16] R.G. Shetkar, A.V. Salker, Mater. Chem. Phys. 108 (2008) 435, doi:10.1016/j.matchemphys.2007.10.022.
[17] S.A.T. Redferm, Phys. Rev. B 48 (1993) 5761.
[18] J. Hanuza, M. Maczka, K. Hernanowicz, P.J. Deren, W. Steck, L. Folcik, H. Drulis, J. Solid State Chem. 148 (1999) 468, doi:10.1006/jssc.1999.8482.
[19] J. Hanuza, M. Maczka, J.H. Ven der Mass, J. Solid State Chem. 117 (1995) 177, doi:10.1006/jssc.1995.1261.
[20] R.L. Frost, L. Duong, M. Weiser, Spectrochem. Acta Part A 60 (2004) 1853, doi:10.1016/j.saa.2003.10.002.
[21] K. Nakamoto (Ed.), Infrared and Raman spectra of inorganic and coordination compounds, John Wiley and Sons, New York, 1980, p. 142.
[22] P.K. Pandey, N.S. Bhave, R.B. Kharat, J. Mater. Lett. 59 (2005) 3149, doi:10.1016/j.matlet.2005.05.018.
[23] A.V. Salker, W. Weisweiler, Appl. Catal. A Gen. 203 (2000) 221, doi:10.1016/S0926-860X(00)00489-0.
[24] M.M. Mohamed, B.M. Abu-Zied, Thermochem. Acta 359 (2000) 109, doi:10.1016/S0040-6031(00)00521-9.
[25] F. Cavani, F. Trifiro, A. Vaccari, Catal. Today 11 (1991) 173, doi:10.1016/0920-5861(91)80068-K.
[26] D. Tichit, M.H. Llhouty, A. Guida, B.H. Chiche, F. Figures, A. Auroux, D. Bartalini, E. Garrone, J. Catal. 151 (1995) 50, doi:10.1006/jcat.1995.1007.
[27] M. Bolognini, F. Cavani, D. Scagliavini, C. Flego, C. Perego, M. Saba, Catal. Today 75 (2002) 103, doi:10.1016/S0920-5861(02)00050-0.
[28] Sung- Ho Cho, J. Park, S. Choi, S. Kim, J. Power Sources 156 (2006) 260, doi:10.1016/j.jpowsour.2005.06.019.
[29] S.M. Gurav, A.V. Salker, Indian J. Chem. Technol. 5 (1998) 286.
[30] A.V. Salker, N.J. Choi, J.H. Kwak, B.S. Joo, D.D. Lee, Sens. Actuators B 106 (2005) 461, doi:10.1016/j.snb.2004.09.008.
[31] L.M. Thang, L.H. Bac, I.V. Driessche, S. Hoste, W.J.M. Van Well, Catal. Today 131 (2008) 566, doi:10.1016/j.cattod.2007.10.038.